



Temperature peak-shift correction methods for NaI(Tl) and LaBr₃(Ce) gamma-ray spectrum stabilisation

R. Casanovas^{a,*}, J.J. Morant^b, M. Salvadó^a

^aUnitat de Física Mèdica, Facultat de Medicina i Ciències de la Salut, Universitat Rovira i Virgili, ES-43201 Reus, Tarragona, Spain

^bServei de Protecció Radiològica, Facultat de Medicina i Ciències de la Salut, Universitat Rovira i Virgili, ES-43201 Reus, Tarragona, Spain

HIGHLIGHTS

- ▶ NaI(Tl) and LaBr₃(Ce) scintillation detectors are used for gamma-ray spectrometry.
- ▶ Environmental temperature changes result in a peak shift and spectral distortion.
- ▶ Two methods are proposed to stabilise the measured spectra.
- ▶ These methods are applied using a software algorithm, without adjusting the gain.
- ▶ Both methods are tested in the laboratory under controlled temperature conditions.

ARTICLE INFO

Article history:

Received 24 February 2012

Received in revised form

26 May 2012

Accepted 1 June 2012

Keywords:

NaI(Tl)

LaBr₃(Ce)

Scintillation gamma-ray spectrometry

Temperature dependence

Peak-shift correction

Spectra stabilisation

ABSTRACT

NaI(Tl) and LaBr₃(Ce) detectors are frequently operated under unstable temperature conditions when used in an open environment. These temperature changes result in a peak shift and spectral distortion during measurement. Two methods are proposed to stabilise the measured spectra; they are applied using a software algorithm, without the necessity of adjusting the gain. Both methods are based on the experimental observation that the relative channel displacement due to temperature changes is approximately the same for all channels. The first method corrects the spectrum using experimental data obtained under controlled conditions in the laboratory, and thus it only depends on the detector temperature. The second method uses one known peak in the spectrum to correct all of the channels: the NORM ⁴⁰K peak for the NaI(Tl) detector, the internal contaminant peak of ¹³⁸La for the LaBr₃(Ce), or an external source when these two cannot be easily identified.

© 2012 Elsevier Ltd. All rights reserved.

1. Introduction

The calibration methodology for NaI(Tl) and LaBr₃(Ce) scintillation detectors in the laboratory is well known (Casanovas et al., 2012). However, when used in an open environment, the detectors frequently operate under unstable temperature conditions. This affects the performance of the detectors either in the crystal itself, such as their light yield or decay time constants (Ilanakiev et al., 2009; Moszyński et al., 2006), or the electronics (ICRU 53, 1994). For environmental monitoring, where the main interest is focused on isotope identification rather than exact activity determination, it is important to account for the effect of temperature on electronics. It is known that temperature changes may lead to gain instabilities and result in a peak shift and spectral distortion during

measurement (ICRU 53, 1994). This can lead to the misidentification of some isotopes.

Several methods are commonly used to stabilise the gain, and thus the gamma-ray spectra. Some examples of this are as follows: using an electronic reference pulse that produces a known equivalent energy in the spectrum (Shepard et al., 1997), attaching an external radioactive source to the detector (Shepard et al., 1997; Pausch et al., 2005), using isotopes from the natural background (Pausch et al., 2005), using the temperature dependence of the light pulse decay time (Pausch et al., 2005) and using LEDs as reference light sources (Pausch et al., 2005; Saucke et al., 2005). However, all of these methods are based on automatically adjusting the gain. Therefore, they are not valid for systems with an analogue gain control.

In this study, we present two methods to correct the peak shift without continuously adjusting the gain. The spectra are corrected by a software implementation of an algorithm that compensates for

* Corresponding author. Tel.: +34 977759382; fax: +34 977759322.

E-mail address: ramon.casanovas@urv.cat (R. Casanovas).

gain drifts due to temperature variations. The methods were tested in the laboratory under controlled temperature conditions. The results indicate that the methods are valid approaches to peak shift corrections in the gamma-ray spectra produced by temperature changes.

2. Materials and methods

2.1. Experimental set-up

The detectors used in this study were a 2" × 2" NaI(Tl) and a 2" × 2" LaBr₃(Ce) scintillation detectors. The NaI(Tl) detector was an ORTEC[®] Model 905-3, and the LaBr₃(Ce) detector was a Brill-LanCe™380 from Saint-Gobain Crystals. Both detectors were coupled to a preamplifier (ORTEC[®] Model 276) and an amplifier (ORTEC[®] Model 575A) with shaping time constants adjusted to 1.5 μs, which were connected to a Multi-Channel pulse-height Analyser (MCA) ORTEC[®] TRUMP™-PCI-2k. The spectrum analysis software that we used was ScintiVision™ from ORTEC[®]. A refrigerator and an oven were used to control the temperature changes, and all of the temperatures were measured using a temperature probe (Brodersen Controls Model PXT-10/11). The experimental data were obtained using four radioactive sources: ¹⁵²Eu, ²⁴¹Am, ¹³⁷Cs and ⁶⁰Co. These sources emit gamma-rays over a range of energies up to 1408 keV.

2.2. Data collection

To validate the methods, we collected two sets of 18 spectra for each detector (72 spectra) in the approximate temperature range of 0 °C to 50 °C, which is the manufacturer's recommended operating range. The first set of spectra was collected using the ¹⁵²Eu source and the second set using a combined source containing ²⁴¹Am, ¹³⁷Cs and ⁶⁰Co. Each spectrum was collected after thermal stability was achieved (at least 1 h of constant temperature), and the corresponding temperature was noted.

2.3. Description of the methods

At a constant reference temperature T_0 (e.g., $T_0 = 25$ °C) of the detector, the position C_{i0} of the i^{th} -channel of the MCA is constant. Thus, the energy calibration is constant. However, temperature changes lead to a channel shift that may invalidate the energy calibration and lead to the misidentification of radionuclides. Thus, the i^{th} -channel position C_{ik} in a gamma-ray spectrum measured at the temperature T_k is displaced with respect to the reference position at T_0 , C_{i0} .

If we assume, for a fixed voltage and gain, that the channel positions only depend on the temperature, we can establish a simple relationship between C_{ik} and C_{i0} :

$$C_{ik} = C_{i0} \cdot f_i(T_k) \quad (1)$$

where $f_i(T_k)$ is a function that depends only on the temperature.

Based on experimental evidence (see Section 3.1), we assume that the relative channel displacement due to temperature changes is approximately the same for all of the N channels conforming the spectrum. Thus, the $f_i(T_k)$ functions become:

$$f_1(T_k) \approx f_2(T_k) \approx \dots \approx f_N(T_k) \equiv f(T_k) \quad (2)$$

To stabilise the spectrum, we displace the C_{ik} channel position to its corrected value $C_{ik}^{\text{corrected}}$, which is the reference position at T_0 , i.e., $C_{ik}^{\text{corrected}} \equiv C_{i0}$.

Using the assumption of Equation (2) in Equation (1), the corrected channel position is given by:

$$C_{ik}^{\text{corrected}} = \frac{C_{ik}}{f(T_k)} \quad (3)$$

With the corrected spectrum, the energy calibration obtained at the reference temperature T_0 is still valid. Thus, the objective of the two proposed methods is to find an approximation to $f(T_k)$ that corrects the measured spectrum.

2.3.1. Method 1

Method 1 corrects the measured spectrum using an algorithm based on previous measurements in the laboratory. Thus, no radioactive or pulse reference is needed during the measurements. However, data must be collected in the laboratory under controlled temperature conditions, which is not always possible.

This method assumes a second-order polynomial approximation to the functions $f_i(T_k)$. Thus, Equation (1) becomes:

$$\frac{C_{ik}}{C_{i0}} = \sum_{j=0}^2 a_{ij} \cdot T_k^j = a_{i0} + a_{i1} \cdot T_k + a_{i2} \cdot T_k^2 \quad (4)$$

The parameters of the second-order polynomial a_{ij} are fit using the 72 spectra (acquired using the different detectors and sources at various temperatures). For each of the main peaks we fit the a_{ij} coefficients. By virtue of Equation (2), we have:

$$a_{1j} \approx a_{2j} \approx \dots \approx a_{Nj} \equiv a_j \quad (5)$$

where a_j is calculated by averaging the a_{ij} coefficients for the N_p peaks considered:

$$a_j \equiv \frac{\sum_{i=1}^{N_p} a_{ij}}{N_p} \quad (6)$$

Equation (4) becomes:

$$\frac{C_{ik}}{C_{i0}} = \sum_{j=0}^2 a_j \cdot T_k^j = a_0 + a_1 \cdot T_k + a_2 \cdot T_k^2 \quad (7)$$

The spectrum is corrected using:

$$C_{ik}^{\text{corrected}} \equiv C_{i0} = \frac{C_{ik}}{\sum_{j=0}^2 a_j \cdot T_k^j} = \frac{C_{ik}}{(a_0 + a_1 \cdot T_k + a_2 \cdot T_k^2)} \quad (8)$$

2.3.2. Method 2

Method 2 uses a single known peak in the spectrum to correct all of the channels. With this method, no previous measurements in the laboratory are needed, and temperature measurements are not required. However, the known peak should be in all of the spectra, either produced by natural background or by an inner contaminant as for the LaBr₃(Ce) detector. If this is not possible, the method requires an external source, which will cause additional undesired counts in the obtained spectra.

This method is based on the assumption made in Equation (2). Thus, it is only necessary to determine $f(T_k)$ for one peak in the spectrum and the spectra can be corrected by following the position of only this one known peak.

Using Equation (3) for the known peak, we have:

$$f(T_k) \equiv \frac{C_{ik}^{\text{known}}}{C_{i0}^{\text{known}}} \quad (9)$$

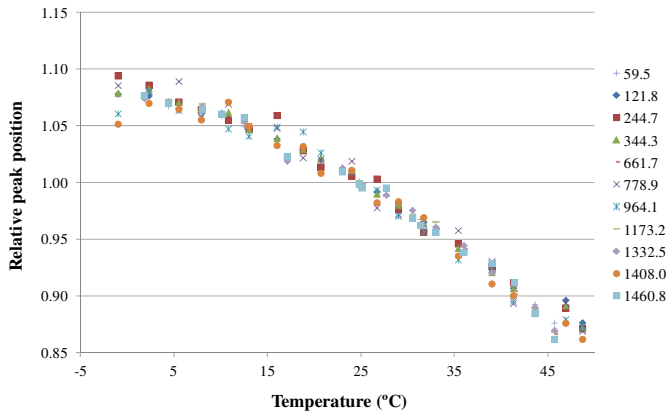


Fig. 1. Relative peak-shift as a function of temperature for the NaI(Tl) detector. The peak positions are normalised to unity at $T_0 = 25\text{ }^\circ\text{C}$ and are named according to their gamma-ray energy in keV.

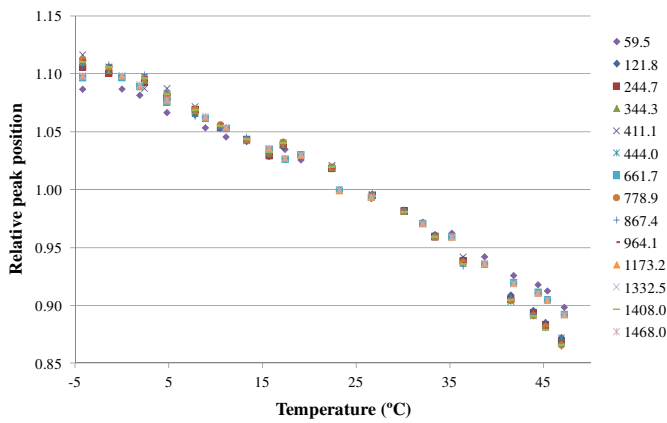


Fig. 2. Relative peak-shift as a function of temperature for the LaBr₃(Ce) detector. The peak positions are normalised to unity at $T_0 = 25\text{ }^\circ\text{C}$ and are named according to their gamma-ray energy in keV.

Combining Equations (3) and (9), all of the channels in the spectrum can be corrected using:

$$C_{ik}^{\text{corrected}} \equiv C_{i0} = C_{ik} \frac{C_{i0}^{\text{known}}}{C_{ik}^{\text{known}}} \quad (10)$$

The spectra of the NaI(Tl) detector were corrected using either the known peak position of the NORM ⁴⁰K or that produced by an external ²⁴¹Am source. For the LaBr₃(Ce) detector, we used the internal contaminant peak from ¹³⁸La present in all of the spectra.

3. Results and discussion

3.1. Temperature dependence of the relative peak positions

Figs. 1 and 2 show the variation in the relative peak positions as a function of temperature for all of the measured isotopes for the NaI(Tl) and the LaBr₃(Ce) detectors, respectively. The data follow the same curve over the range of temperatures studied. Therefore, the assumption made in Equation (2) is reasonable and feasible. The temperature dependence of the relative peak positions is approximately the same for all channels in the spectrum. Despite the different temperature dependences of the studied crystals (Moszyński et al., 2006), no significant differences are observed between the peak shifts in the NaI(Tl) and the LaBr₃(Ce) detectors. Thus, it suggests that the main component of instability is caused by photomultipliers when the temperature changes affect all the detection system.

3.2. Validation of method 1

To test the validity of method 1, for each detector we used the data of one set of measurements to correct the other set. Specifically, we took the data obtained from the second source (²⁴¹Am + ¹³⁷Cs + ⁶⁰Co) to correct the spectra obtained with the first source (¹⁵²Eu) and vice versa. Figs. 3 to 6 compare the waterfall plots (top) for the uncorrected and corrected spectra for both

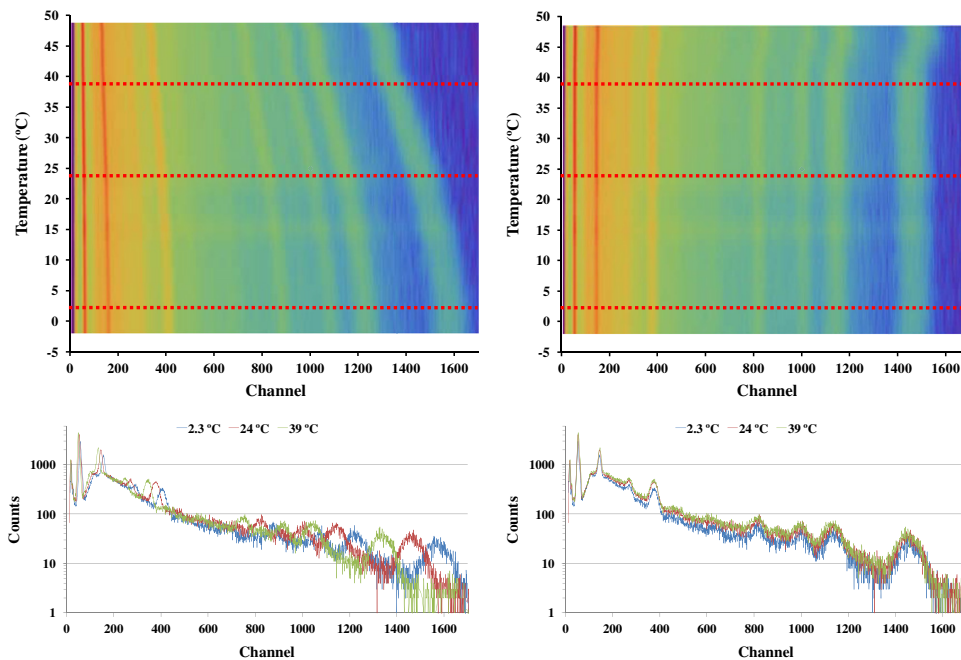


Fig. 3. ¹⁵²Eu spectra as a function of temperature for the NaI(Tl) detector. The raw measured spectra (left) are corrected (right) using the data obtained from the source composed of ²⁴¹Am, ¹³⁷Cs and ⁶⁰Co. The red dotted lines on the waterfall plots (top) indicate which pulse height spectra (bottom) are represented by way of example. (For interpretation of the references to colour in this figure legend, the reader is referred to the web version of this article.)

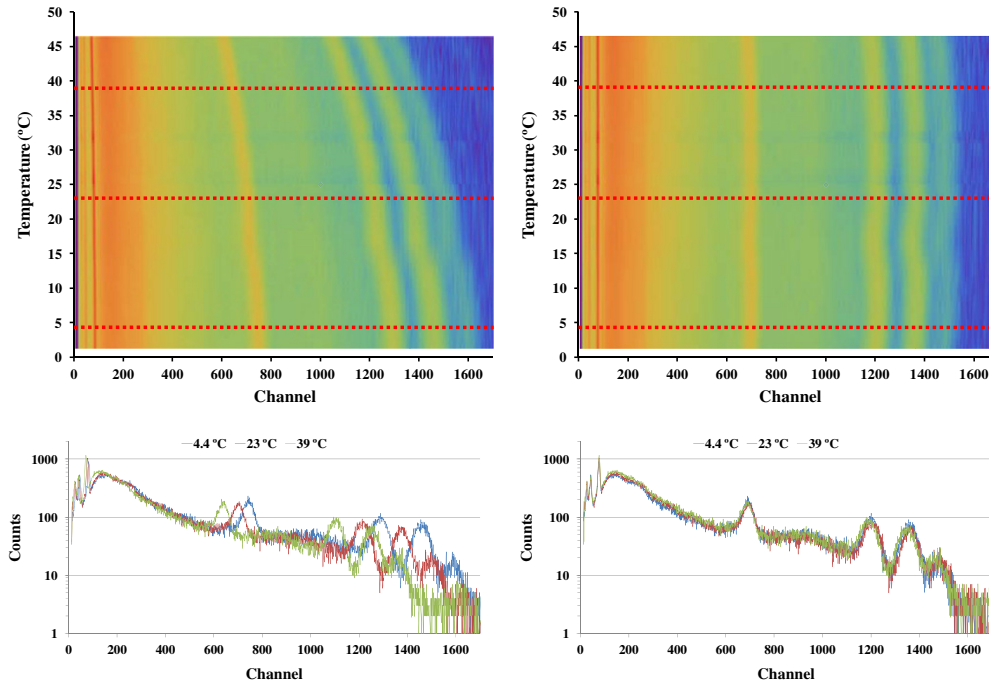


Fig. 4. ^{241}Am , ^{137}Cs and ^{60}Co spectra as a function of temperature for the NaI(Tl) detector. The raw measured spectra (left) are corrected (right) using the data obtained from the ^{152}Eu source. The red dotted lines on the waterfall plots (top) indicate which pulse height spectra (bottom) are represented by way of example. (For interpretation of the references to colour in this figure legend, the reader is referred to the web version of this article.)

detectors. In these spectra, the horizontal axis represents the channel number, the vertical axis the temperature at acquisition and the colour scale indicates the logarithm of the pulse height, which is red for higher values and purple for lower ones. By way of example, some pulse height spectra (bottom) are also represented at different temperatures, which are marked with a red dotted line on the waterfall plots.

The corrected spectra obtained using method 1 are, in general, stable. The corrected peak positions are significantly more constant against temperature variations. The largest discrepancies between the corrected peak positions and the reference peak positions occur at the extremes of the temperature. The method performs well between 0 °C and 40 °C, which is the normal operating range for the detectors. The fluctuations observed in Figs. 3 to 6 near 15 °C are

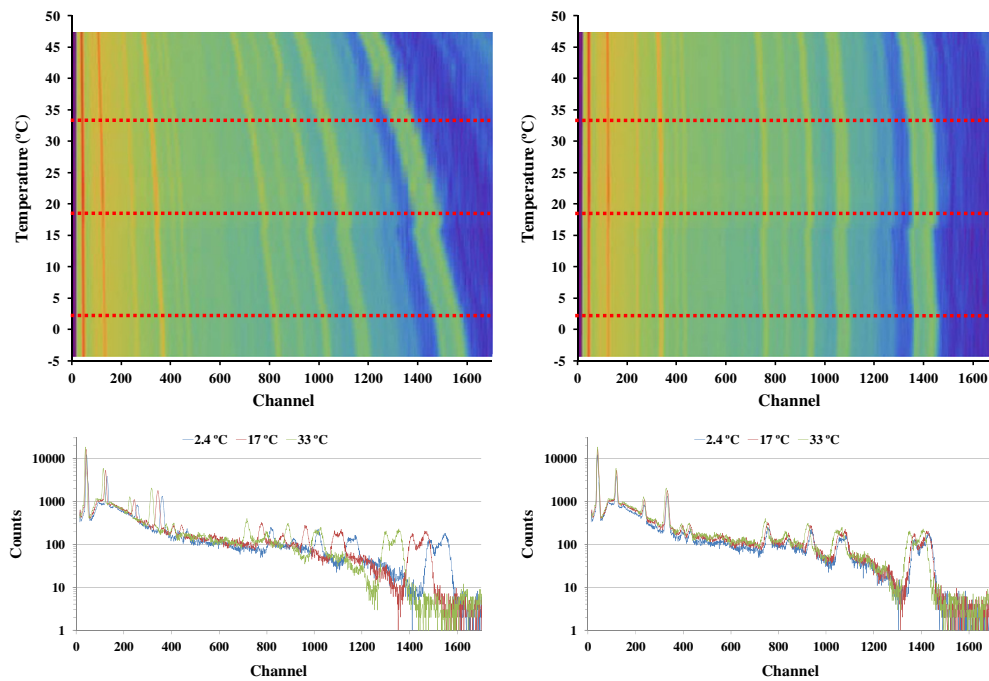


Fig. 5. ^{152}Eu spectra as a function of temperature for the LaBr₃(Ce) detector. The raw measured spectra (left) are corrected (right) using the data obtained from the source composed of ^{241}Am , ^{137}Cs and ^{60}Co . The red dotted lines on the waterfall plots (top) indicate which pulse height spectra (bottom) are represented by way of example. (For interpretation of the references to colour in this figure legend, the reader is referred to the web version of this article.)

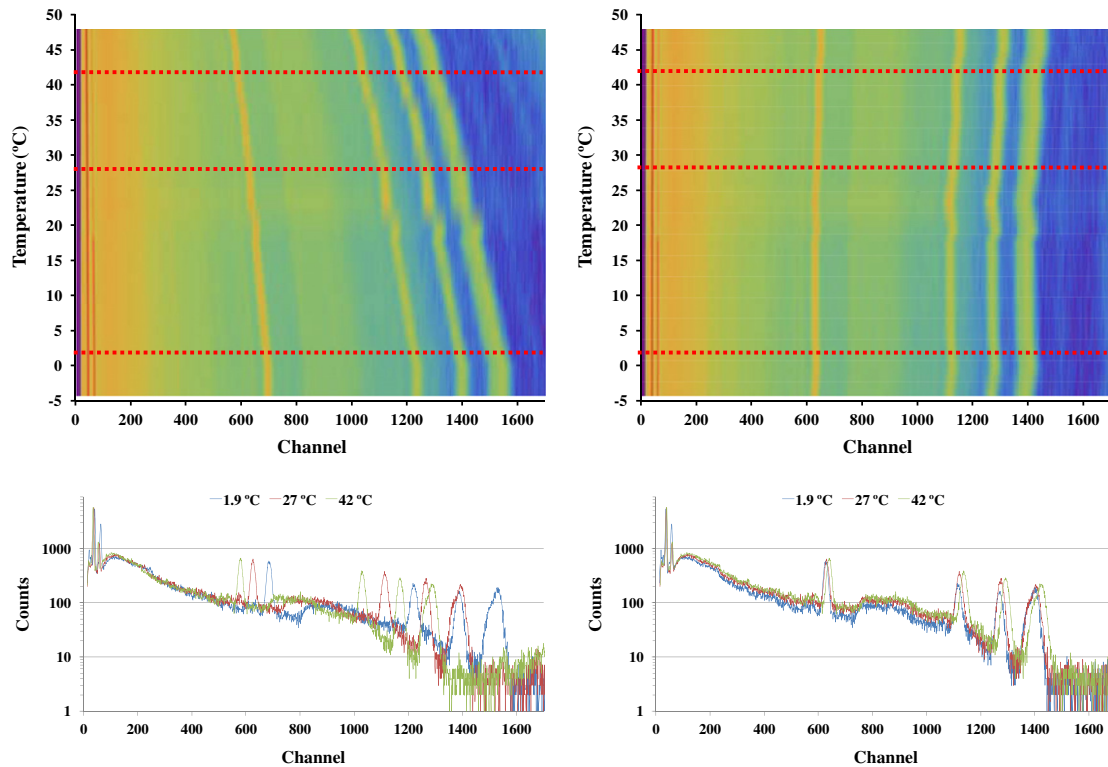


Fig. 6. ^{241}Am , ^{137}Cs and ^{60}Co spectra as a function of temperature for the $\text{LaBr}_3(\text{Ce})$ detector. The raw measured spectra (left) are corrected (right) using the data obtained from the ^{152}Eu source. The red dotted lines on the waterfall plots (top) indicate which pulse height spectra (bottom) are represented by way of example. (For interpretation of the references to colour in this figure legend, the reader is referred to the web version of this article.)

due to the transfer of the detectors from the refrigerator to the oven. However, the spectra correction in the environment will not be affected by this phenomenon because the fitting functions are soft and this fluctuation is due to a problem in data collection in the laboratory. Further measurements should be performed using a better environmental chamber.

After testing method 1, we used the data of the two sets of measurements to correct all of the spectra. Figs. 7 and 8 show the relative deviation of the corrected peak positions with respect to the reference position for the $\text{NaI}(\text{Tl})$ and the $\text{LaBr}_3(\text{Ce})$ detectors, respectively.

The spread of points observed at the extremes of the studied temperatures could be attributed to some kind of thermal inertia

in the detectors. In fact, it can be observed in Figs. 1 and 2 that the measurements with the first source of ^{241}Am , ^{137}Cs and ^{60}Co have a slightly different tendency that those obtained with the second one of ^{152}Eu . This is more pronounced in Fig. 2 for the $\text{LaBr}_3(\text{Ce})$, where a bifurcation between the first and the second source can be observed at the extremes of temperatures. However, the differences are, in absolute value, less than 3% in the temperature range of $-5\text{ }^\circ\text{C}$ and $50\text{ }^\circ\text{C}$ and a smaller relative deviation (below 2% in absolute value) in the normal operating range of $0\text{ }^\circ\text{C}$ to $40\text{ }^\circ\text{C}$, which is an acceptable correction for both detectors. These figures also validate that the relative channel displacement due to temperature changes is approximately the same for all channels.

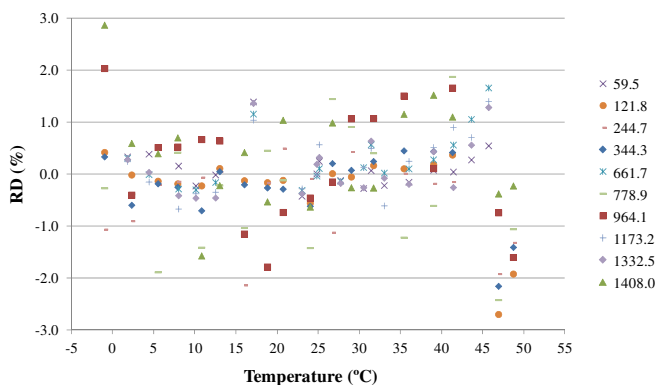


Fig. 7. Relative deviation ($\text{RD}(\%) = (C_{i0} - C_{ik})/C_{i0} \cdot 100$) of the corrected peak positions as compared to their reference positions for the $\text{NaI}(\text{Tl})$ detector. The correction was calculated using all of the data shown in Fig. 1. The peaks are named according to their gamma-ray energy in keV.

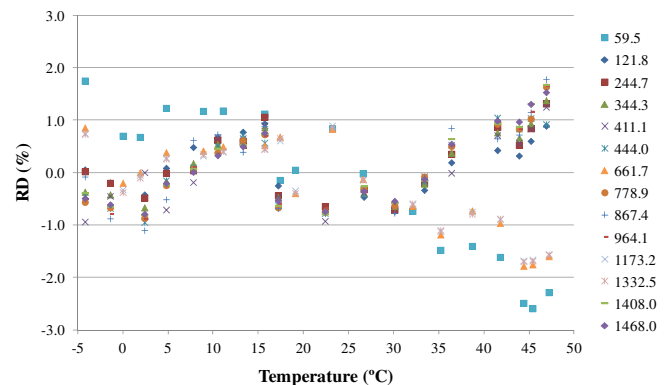


Fig. 8. Relative deviation ($\text{RD}(\%) = (C_{i0} - C_{ik})/C_{i0} \cdot 100$) of the corrected peak positions as compared to their reference positions for the $\text{LaBr}_3(\text{Ce})$ detector. The correction was calculated using all of the data shown in Fig. 2. The peaks are named according to their gamma-ray energy in keV.

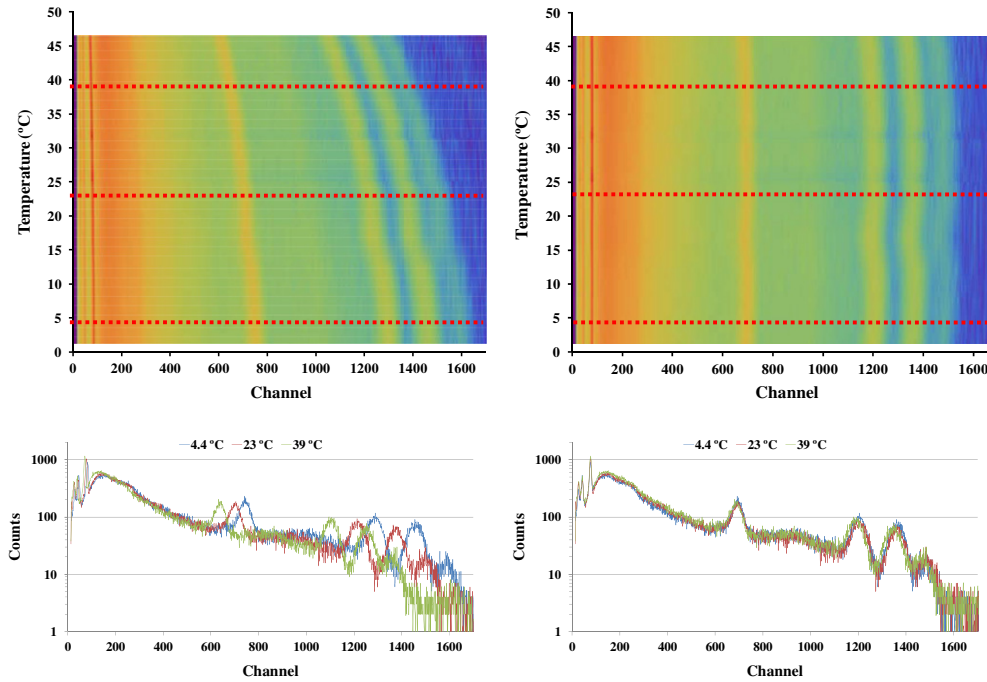


Fig. 9. ^{241}Am , ^{137}Cs and ^{60}Co spectra as a function of temperature for the NaI(Tl) detector. The raw measured spectra (left) are corrected (right) using the data obtained from the NORM ^{40}K peak. The red dotted lines on the waterfall plots (top) indicate which pulse height spectra (bottom) are represented by way of example. (For interpretation of the references to colour in this figure legend, the reader is referred to the web version of this article.)

3.3. Validation of method 2

3.3.1. NaI(Tl) spectrum correction using ^{40}K peak

Fig. 9 shows the correction of the $^{241}\text{Am} + ^{137}\text{Cs} + ^{60}\text{Co}$ spectrum using the ^{40}K peak. The quality of the correction depends on the quality of the ^{40}K peak. The correction is acceptable over the range

of temperatures. The ^{40}K content in the laboratory is small compared to the environment; the method is expected to perform better when used outdoors.

Unfortunately, this method cannot be used when the reference peak cannot be identified, either due to low activity or low detector resolution. The latter is why the ^{152}Eu spectrum cannot be

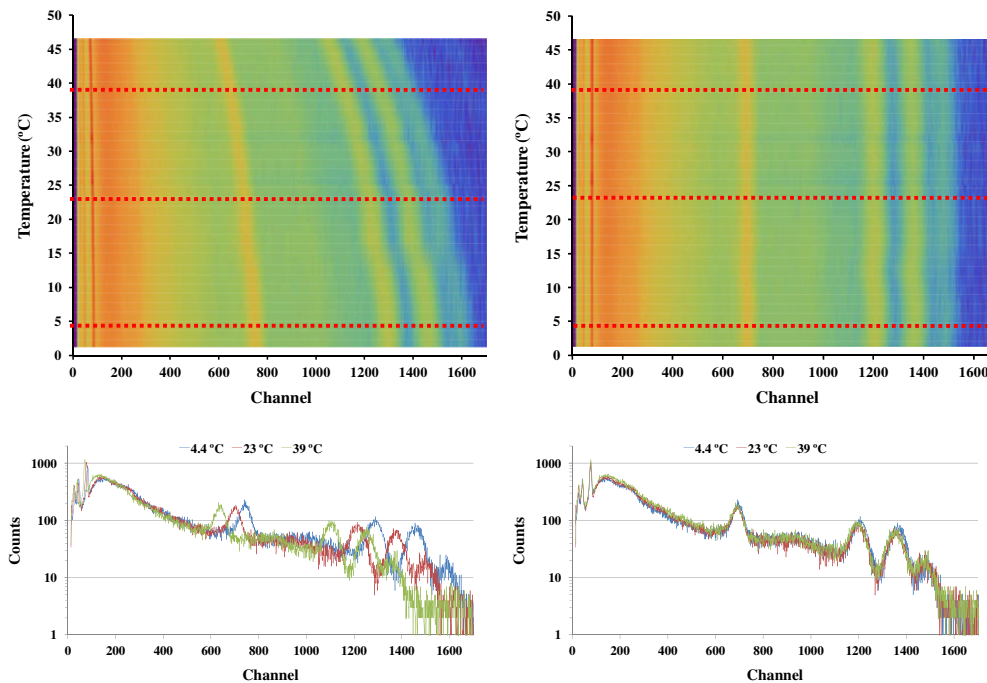


Fig. 10. ^{241}Am , ^{137}Cs and ^{60}Co spectra as a function of temperature for the NaI(Tl) detector. The raw measured spectra (left) are corrected (right) using the data obtained from the ^{241}Am peak. The red dotted lines on the waterfall plots (top) indicate which pulse height spectra (bottom) are represented by way of example. (For interpretation of the references to colour in this figure legend, the reader is referred to the web version of this article.)

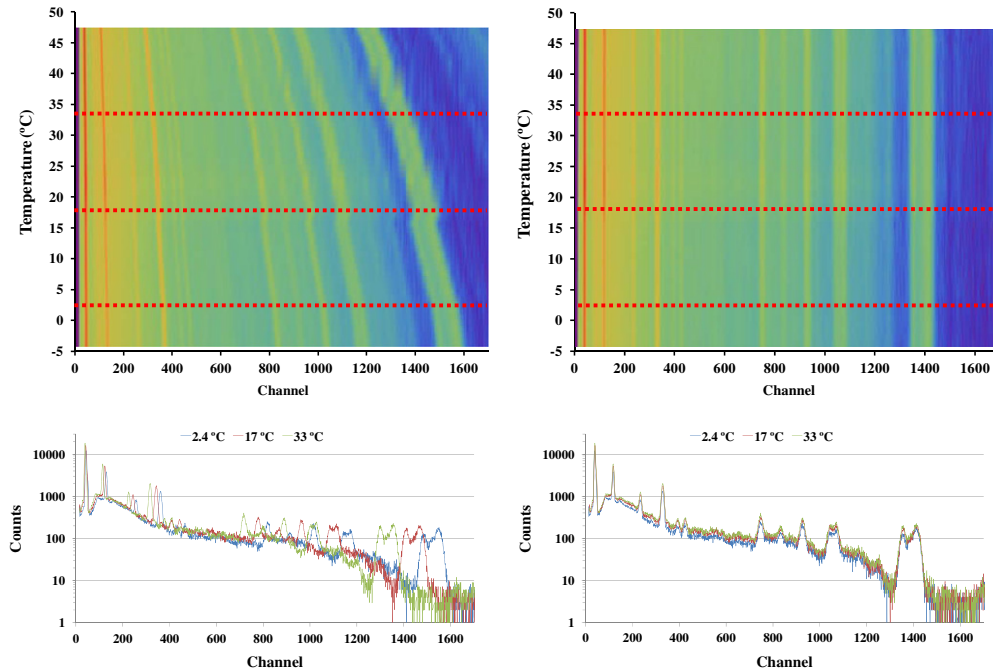


Fig. 11. ^{152}Eu spectra as a function of temperature for the $\text{LaBr}_3(\text{Ce})$ detector. The raw measured spectra (left) are corrected (right) using the data obtained from the ^{138}La internal contaminant peak. The red dotted lines on the waterfall plots (top) indicate which pulse height spectra (bottom) are represented by way of example. (For interpretation of the references to colour in this figure legend, the reader is referred to the web version of this article.)

corrected by this method. In this case, the ^{40}K peak is hidden by the ^{152}Eu 1408 keV peak.

3.3.2. $\text{NaI}(\text{Tl})$ spectrum correction using ^{241}Am peak

The previous $\text{NaI}(\text{Tl})$ spectra corrected using ^{40}K are not accurate enough due to the peak quality, which depends on the concentration of potassium in the environment. To overcome this, it is necessary to add an external radioactive source to the detector. To

avoid peak interferences, the source should not emit gamma-rays in the energy range of interest. In our case, ^{241}Am was used as an external source, adding extra counts only in the spectra below 60 keV. Thus, the spectra may be trusted only above this energy if no extra analysis is performed. In Fig. 10 we show the correction of the $^{241}\text{Am} + ^{137}\text{Cs} + ^{60}\text{Co}$ spectrum using the ^{241}Am peak. Because the ^{241}Am peak is better identified than the ^{40}K peak, the correction is more stable.

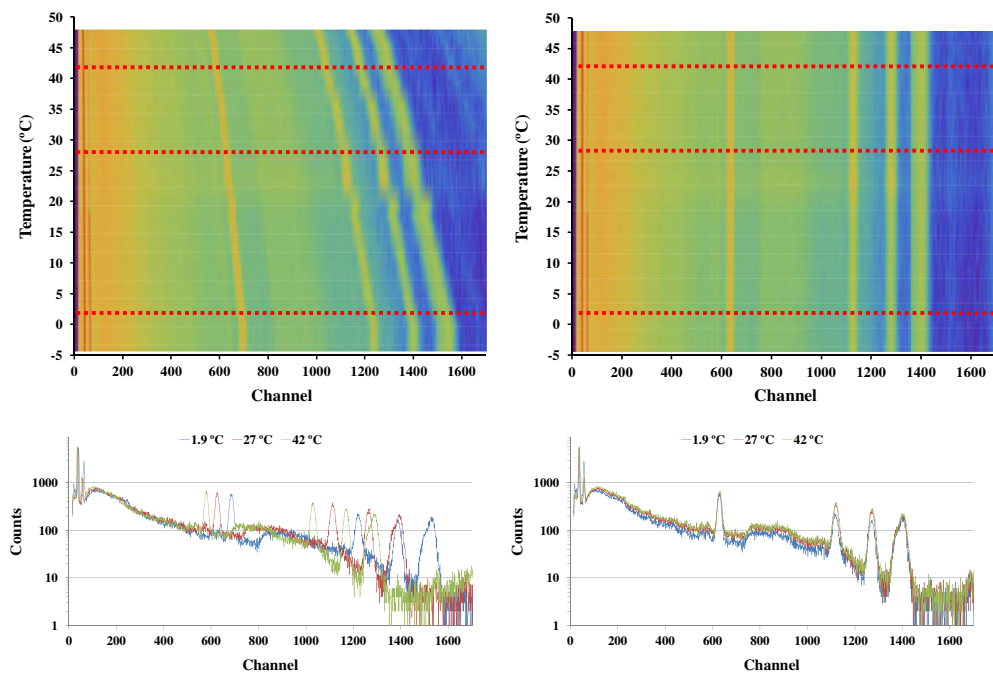


Fig. 12. ^{241}Am , ^{137}Cs and ^{60}Co spectra as a function of temperature for the $\text{LaBr}_3(\text{Ce})$ detector. The raw measured spectra (left) are corrected (right) using the data obtained from the ^{138}La internal contaminant peak. The red dotted lines on the waterfall plots (top) indicate which pulse height spectra (bottom) are represented by way of example. (For interpretation of the references to colour in this figure legend, the reader is referred to the web version of this article.)

3.3.3. $\text{LaBr}_3(\text{Ce})$ spectra correction using ^{138}La internal contamination

The internal contaminant of the $\text{LaBr}_3(\text{Ce})$ detector can be used for spectrum stabilisation. Figs. 11 and 12 show the ^{152}Eu and $^{241}\text{Am} + ^{137}\text{Cs} + ^{60}\text{Co}$ spectra stabilised using the ^{138}La peak. The usual disadvantage of radioactive contamination plays a positive role in spectrum stabilisation.

4. Conclusions

In this study, we presented two methods to correct the peak shift that do not require adjustment of the gain. Thus, both methods are useful to stabilise gamma-ray spectra obtained under unstable temperature conditions.

The first method provides spectrum stabilisation in the absence of known peaks, especially when alternative methods are not available. However, it requires some measurements under controlled temperature conditions, which cannot always be performed and may be specific to each detector. Besides, some internal thermal inertia are observed, worsening the peak-shift correction. Even so, the results show a relative deviation of less than 2%, in absolute value, in the peak correction in the normal operating range of 0 °C to 40 °C for both detectors.

The second method does not require previous measurements in the laboratory, so it can be generally applied. In addition, it provides better results than method 1 since the thermal inertia do not affect the corrections. However, this method depends on a known peak in all of the spectra, which is not always available or identifiable, especially in the $\text{NaI}(\text{Tl})$ detector. For the $\text{LaBr}_3(\text{Ce})$ detector, the internal contaminant, ^{138}La , together with the better energy resolution of the detector, make it easy to apply this method.

The second method can also be applied using an external radioactive source (for example, ^{241}Am). This is especially useful to stabilise the $\text{NaI}(\text{Tl})$ spectra in environments with low ^{40}K content. However, adding an external radioactive source causes undesired counts in the spectra. Fortunately, they can be minimised using mechanical devices to shield the source when it is not in use.

Both methods were tested under stable temperature conditions that may not reflect real scenarios in the environment. Additionally, when used in an open environment, both methods are applied by software after the spectra acquisition (instead of adjusting the gain during the measurements). For these reasons, it is desirable to use short integration times (e.g., 10 min) during the spectra acquisition and correct the spectra after each integration.

We recommend using method 2 as the default method and implementing method 1 only when the known peak cannot be identified or is not significant (usually in $\text{NaI}(\text{Tl})$ detectors). When the known peak cannot be detected, it is possible to implement the second method by adding an external radioactive source.

Finally, these methods cannot replace the conventional methods used with digital systems. In fact, in analogue systems, the number of available channels decreases when the temperature rises, and resolution may be lost. This should not be a problem for MCA with a large number of channels, but it is an important distinction between the analogue and digital correction methods.

References

- Casanovas, R., Morant, J.J., Salvadó, M., 2012. Energy and resolution calibration of $\text{NaI}(\text{Tl})$ and $\text{LaBr}_3(\text{Ce})$ scintillators and validation of an EGS5 Monte Carlo user code for efficiency calculations. *Nucl. Inst. Meth. Phys. Res. A* 675, 78–83.
- Ianakiev, K.D., Alexandrov, B.S., Littlewood, P.B., Browne, M.C., 2009. Temperature behaviour of $\text{NaI}(\text{Tl})$ scintillation detectors. *Nucl. Instrum. Methods. Phys. Res. A* 607, 432–438.
- ICRU 53, 1994. Gamma-ray Spectrometry in the Environment. International Commission on Radiation Units and Measurements, Bethesda, Maryland. Report 53.
- Moszyński, M., Nassalski, A., Syntfeld-Kazuch, A., Szczęśniak, T., Czarnacki, W., Wolski, D., Pausch, G., Stein, J., 2006. Temperature dependences of $\text{LaBr}_3(\text{Ce})$, $\text{LaCl}_3(\text{Ce})$ and $\text{NaI}(\text{Tl})$ scintillators. *Nucl. Instrum. Methods. Phys. Res. A* 568, 739–751.
- Pausch, G., Stein, J., Teofilov, N., 2005. Stabilizing scintillation detector systems by exploiting the temperature dependence of the light pulse decay time. *IEEE Trans. Nucl. Sci.* 52, 1849–1855.
- Saucke, K., Pausch, G., Stein, J., Ortlepp, H.G., Schotanus, P., 2005. Stabilizing scintillation detector systems with pulsed LEDs: a method to derive the LED temperature from pulse height spectra. *IEEE Trans. Nucl. Sci.* 52, 3160–3165.
- Shepard, R., Wawrowski, S., Charland, M., Roberts, H., Möslinger, M., 1997. Temperature stabilization of a field instrument for uranium enrichment measurements. *IEEE Trans. Nucl. Sci.* 44, 568–571.